Journal of Information Systems Engineering and Management
2025, 10(4)
e-ISSN: 2468-4376
https://www.jisem-journal.com/

Research Article

Efficient Load Balanced Routing based Trusted Clustering to Maximizing Network Lifetime in Heterogeneous Wireless Sensor Networks using Distributed Compressive Sensing Technique

Mr. Dhananjay Arun Kumbhar[1], Dr. R R Dube[2]

[1] *Assistant Professor, School of Engineering and Technology, Sanjivani University, Kopargaon, Maharashtra India.*
(Corresponding Author: dhananjay.kumbhar@gmail.com)

[2] *Professor, Department of Electronics and Telecommunication Engineering, Walchand Institute of Technology, MH, India.*
(rajendradube67@rediffmail.com)

ARTICLE INFO

Received: 15 Dec 2024

Revised: 25 Jan 2025

Accepted: 05 Feb 2025

ABSTRACT

Wireless Sensor Networks (WSNs) face significant challenges in energy efficiency, load balancing, and data transmission. To address these, we propose the Efficient Load Balanced Routing based Trusted Clustering to Maximize Network Lifetime using Distributed Compressive Sensing (ELRC-DCS) approach. This method employs a hierarchical network model with sensors organized in a bi-layer and a static data sink positioned centrally. Optimized Cluster Head (CH) selection ensures balanced power consumption, enhanced load distribution, and energy efficiency by avoiding low-energy nodes and traffic congestion. The model incorporates a Distributed Compressive Sensing Technique (DCST) to reduce energy consumption and simplify data transmission, while a trust mechanism ensures secure and reliable node-to-node communication. This trust mechanism evaluates direct, indirect, and new trust values to improve data reliability and prevent malicious behavior. The ELRC-DCS approach optimizes clustering, balances energy usage, minimizes communication expenses, and guarantees reliable data transmission, resulting in enhanced network durability. Simulation results demonstrate that ELRC-DCS significantly outperforms existing models (CACIACA, OCCMPHE, and EMRHPFC), achieving the lowest communication delay (108.30 ms) and the highest energy efficiency (93.45%). Additionally, ELRC-DCS achieves a data success rate of 91.64%, network throughput of 784.26 Kbps, and reduced routing overhead with only 898 packets. These results position ELRC-DCS as a robust and efficient solution for large-scale WSN deployments in environmental monitoring applications, offering superior energy efficiency, reliability, and communication quality compared to traditional methods.

Keywords: Load Balancing, Heterogeneous Wireless Sensor Networks (HWSN), Cluster Head (CH), and Distributed Compressive Sensing Technique (DCST)

1. INTRODUCTION:

Wireless sensor networks (WSN) have become a prominent topic of research as e.g., used in industrial applications [1] and in everyday uses such as smart grids [2], security monitoring [3] or risk prevention [4]. The battery life of mobile sensors depends on the power supplied to the sensor from an external source; other energy supply methods are employed to avoid unnecessary energy consumption. Included in these techniques are software, power management, and efficient routing. Multi-hop design is employed in routing protocols to prevent the direct transmission of packets from sensors to data sinks [5]. Two variations of it are flat routing and hierarchical routing. Planar routing involves determining the routes from sensors to sinks that are the shortest. The use of short communication distances results in decreased energy usage. With the routing protocol, packets are clustered together into clusters, with each CH combining packet data to reduce redundancy and improve the node's lifespan [6].

Providing sensor data for transmission to a base station via WAN is not as expensive as possible due to the need for high communication costs [7]. However, this technique is constrained by the Niquist–Shannon theorem which states that to retrieve compressed data, the sampling rate (N) must be doubled in frequency. Typically, WSNs that are limited in resources require multiple instances. In addition, compression methods and defining large coefficients can be difficult. To overcome these limitations, pressure has been considered [8]. The concept of CS is designed to reconstruct small or small signals using only a few measurements, without knowledge of the signal structure [9]. This approach is beneficial when signals are sparse on a known basis, sensor computations are costly, and receiver computations are inexpensive - all of which align with WSNs [10]. Compared to data compression, implementing compressive sensing in WSNs shows potential for significant improvements as it does not require encoding at low-power sensor nodes.

1.1 Research contribution:

A routing system that utilizes energy, an innovative ELRC-DCS framework that incorporates check-list and multi-hop routing. Efforts such as this are effective in balancing energy consumption in cell nodes, prolonging network life, and optimizing resource usage in WSNs. To decrease costs associated with data transfer, DCST integration is implemented due to pressure. It reduces the energy required for communication by reconstructing data from smaller measurements, thereby increasing energy conservation and transmission efficiency in resource-constrained WSN environments. Trust-based security is a robust means of ensuring secure and reliable data transmission across multiple nodes. By assessing the impact of direct, indirect, and innovative trust values, this model enhances data reliability, reduces security risks, and safeguards against malicious activity in WSNs. Enhanced network performance and integration, leading to more energy conservation, extended network life, and reliable data transfer. The proposed ELRC-DCS model is adaptable to large-scale WSN applications and can be used for practical purposes such as monitoring environmental conditions. The organization of the paper Section 1 explains the previous model techniques and drawbacks, section 2 explains in detail the previous works, section 3 introduces the ELRC-DCS proposed model in detail, Sections 4 and 5 explain detailed about the simulation parameters for the ELRC-DCS model, and following section 6 is a conclusion.

2. RELATED WORKS:

In [11], it incorporates a reservation and routing algorithm coupled with data aggregate on a threshold for various WSNs to minimize redundant transmission of data. The model prevents redundant transmissions and improves energy efficiency by using threshold-based conditions. The proposed multi-hop model enhances load balancing and reduces end-to-end delay compared to protocols like TSEP, TDEEC, LEACH, and TEEN, ensuring better network stability. In [12], the use of GWO is being explored as an alternative approach to optimize urban WSNs for sustainable scheduling, while also improving network reliability and energy efficiency. IGWO is compared to GWO and other methods and shows better performance in reducing cluster heads, gateways, and dead nodes. The algorithm's convergence is demonstrated in a large-scale WSN with 500 sensors and 50 cluster heads, showing significant improvements. In [13], an ERCP for WSNs optimizes energy savings and reliable data delivery using metrics like link quality, energy, and distance. Experimental results show that ERCP outperforms recent algorithms in homogeneous and heterogeneous networks. In [14], active aggregates are utilized as the cell head and spanning tree for data transmission in the proposed LB-TBDAS tree-driven data collection scheme for grid-bound WSNs. LB-TBDAS has the potential to reduce energy consumption and increase network lifetime, which is over 100% less than that of GB-PEDAP and PEDAH, while also addressing connection issues. In [15], using K-means and dynamic canopy optimization, the DCK-LEACH algorithm is used to select WSNs with dual cluster heads for energy conservation. If the strength and distance of the cluster center are factors, they select one over another; if that fails, then the selection follows. The second cluster head is chosen by its strengths and proximity to the base station. Simulation results indicate that DCK-LEACH outperforms existing techniques in terms of node-capacity latency and network latency. In [16], the EEDC scheme and RHCER are utilized in WSN-IoT scenarios to improve energy efficiency and load balancing. According to simulation results, EEDC achieves a 31% decrease in energy consumption and an increase in packet loss ratio by 30% when compared to current methods. In [17], to optimize data collection, Sequential Convex Approximation (SCA) and mobile sink are utilized in the TPEMLB approach to balance energy consumption across nodes and improve load distribution. By using this model, the network's longevity is greatly improved, energy consumption is reduced, and performance is ensured to be better than with other methods. In [18], a GA and SCHSM optimize energy usage in IoT-enabled WSNs by considering factors like distance, node energy, and density. Multi-mobile synchronous nodes reduce energy consumption and increase network life by improving communication continuity. In [19], to address the challenges of load balancing in cloud computing, adopt a metaheuristic approach that prioritizes optimization over other approaches and improves performance migration, response time management, output control, and error prevention. This approach makes it easier to explore and use, avoids local optimization, and evaluates its performance with benchmark algorithms using Cloud Sim. In [20], a clustering-based algorithm to improve the quality of the service and energy efficiency in WSNs, addressing sensor limitations like battery size. MATLAB simulations show proposed algorithm outperforms existing clustering protocols such as LEACH and SEP. In [21], the utilization of UWASN, a multi-layer approach in underwater acoustic sensor networks, tackles load balancing and dynamic network mechanisms while dealing with MAC and routing layers. The proposed system using reinforcement learning for slot time allocation and artificial fish filtering integrated with a bacterium feeding algorithm for energy-aware QoS routing shows better performance compared to current trends. In [22], focusing on trust-based security to identify and mitigate the impact of malicious sensor devices while balancing load among cluster heads. SLBR offers improved energy efficiency, reduced communication overhead, and better throughput compared to the Exponential Cat Swarm Optimization (ECSO) model. Experimental results demonstrate that SLBR enhances network lifetime and decreases misclassification rates of malicious sensors, achieving superior overall performance. In [23], enhanced cluster head selection, data redundancy, and link creation are achieved by enterprise WSNs through the use of redundant and redundant redundancy. Simulation results indicate that DDCS significantly reduces data transmission, energy consumption at cluster heads, and overall network delay compared to traditional DCS. In [24], enhancing energy efficiency and prolonging network lifetime. by utilizing a distinct cross-modification search policy, EOR-iABC determines which cluster head to optimize and improves local search strategies using worker and observer phases. Based on simulation results, EOR-iABC is 27% more efficient than the OCABC scheme, and 16% more effective than the IABCOCT scheme. In [25], enhance network lifetime by performing dimensionality reduction at transmitter and signal reconstruction at receiver using a greedy method. Performance evaluations reveal the effectiveness of the greedy method in terms of reconstruction success and error rates, assessed with varying data sparsity and applied to real temperature and humidity datasets. In [26], wireless sensor networks employ a pressure relief technique to obtain energy-efficient data by gauging the spatial correlation between adjacent stations. By utilizing Bayesian inference and belief propagation for signal recovery, the proposed method demonstrates improved reconstruction accuracy and reduced energy consumption compared to existing techniques. In [27], by utilizing techniques such as ant colony optimization and cuckoo search, the BACREED algorithm optimizes data acquisition and routing in WSNs to improve network reliability and energy efficiency. Simulation results show an 84% reduction in path length and enhanced performance compared to baseline algorithms, highlighting the effectiveness of the integrated FELACS-ODR data compression scheme. In [28], it is an EDAS, of WSN wireless sensor networks, using an I-LEACH algorithm that selects the best cluster head while reducing data integrity via network encryption. Simulation results show that EDAS effectively reduces energy consumption and increases network performance compared to existing data aggregation techniques. In [29], a Convolutional Neural Network combined with Fuzzy Logic (CNN-FL) to effectively identify and categorize trustworthy and malicious nodes in Wireless Sensor Networks (WSNs). By integrating this with a Neuro Genetic Optimizer-based routing strategy built on the LEACH protocol, the method enhances data transmission security while significantly reducing latency and energy consumption, outperforming existing protocols in key performance metrics. In [30], the dynamic data aggregation technique for WSNs optimizes energy consumption by dynamically deciding whether to aggregate data at cluster heads or transmit it directly to the sink based on hop counts. By utilizing metrics like error rate and queue length to select cluster heads, data aggregation efficiency and the network's overall performance are enhanced in comparison to previous algorithms. In [31], to enhance energy efficiency in WSNs by reducing data size during transmission. By addressing issues like outlier detection and optimizing encoding methods, the proposed enhancements lead to significant energy savings and improved data accuracy, making these techniques highly beneficial for energy-constrained applications requiring reliable data integrity.

3. PROPOSED ELRC-DCS TECHNIQUE

Energy-efficient routing in WSNs is made possible by the proposed ELRC–DCS approach, which employs optimal CH selection considering factors such as distance and traffic load, as well as levels of energy consumption. electricity. Trust analysis includes direct, indirect, and innovative trust assessments for secure communication within and between clusters. By utilizing compression, it can recover dispersed signals and lower the expenses of transmitting data. This method automatically selects the most efficient relay nodes to balance the network load and maximize lifetime. DCST improves the ability to get information by propagating beliefs in factor graphs.

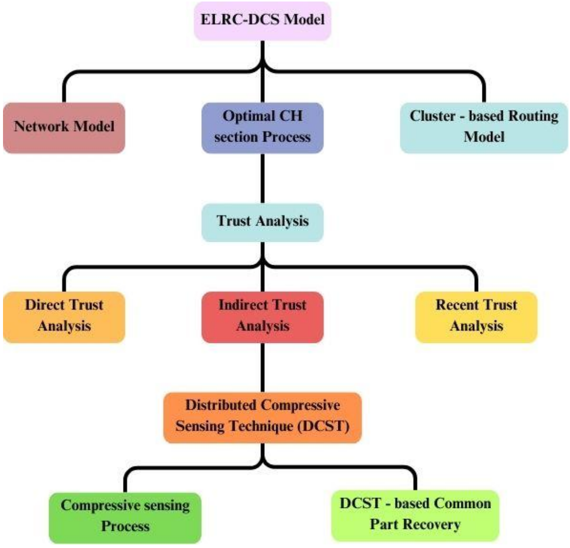
ELRC-DCS Model
Network Model
Optimal CH section Process
Cluster - based Routing Model
Trust Analysis
Direct Trust Analysis
Indirect Trust Analysis
Recent Trust Analysis
Distributed Compressive Sensing Technique (DCST)
Compressive sensing Process
DCST - based Common Part Recovery

Figure 1 - Proposed ELRC-DCS

3.1 Network Model:

The network model assumes that all sensors are evenly distributed within an R region with a radius of d. In this model, the center of each sensor in the cluster receives its data sink from somewhere outside the network. These sensors send their detected packets to their CH, aggregate them, and send them to the data sink via the shortest path. The probability of rotating the CHs in each cluster is ensured to be equal for all sensors. Additionally, all sensors possess identical initial energy levels (E_{init}). The network employs sensors to collect a range of environmental parameters, including humidity, temperature, and air quality. By merging these parameters, they are transmitted to the sink through CHs in a transmission path. In a data cycle, CH u sends and receives m packets to the sink. Each data cycle contains the CH's p_k, which merges the kth event and produces g_k packets. The calculation of the production rate (r) for each CH u in every data cycle is as follows:

$$r_u = \sum_{k=1}^{m} p_k g_k \qquad (1)$$

To make the power computation model less complicated, the primary factor to consider is the transmission power in the path loss model. This is because it consumes more power compared to reception and idle scenarios. $P_M(r_u)$ is the unit of measurement for power in multi-hop transmission. The lifespan of a CH user node can be depicted in this manner:

$$N(u) = \frac{E_{init}}{P_M(r_u)} \qquad (2)$$

The starting battery capacity for each sensor is referred to as E_{init}, and the lifecycle is the period between placing the sensors in the network and when the first sensor's battery capacity is exhausted.

3.2 Optimal CH Section Process:

It is assumed that N nodes are distributed in an area of $A = R \times R$ square meters. For simplicity, we will say that the sink is in the middle of this area. $r_p(r_p \leq d_0)$ is the minimum distance at which each node from its BS or CH can transmit, with a maximum of d_0 being the range. We assume that after initialization, a "hello" (BS) message is sent to all nodes at the specified power level. The distance (D_i) between the BS and each node can be estimated by using the strength of the received signal. The BS D_{avg} is determined by the following method to determine the average distance between nodes:

$$D_{avg} = \frac{1}{N}\sum_{i=1}^{N} D_i, \quad (3)$$

An approximate value for D_{avg} depends on the model for the energy consumed by the CH in the circle and the average distance between each group (d_{CH}), as well as the corresponding average ranges from one to the other. The number of clusters, C; the compressed data, Y. The calculation of energy transfer from a non-CH node is as follows:

$$D_{avg} \approx d_{CH} + d_{BS} \quad (4)$$

$$E_{CH} = \left(\frac{N}{C} - 1\right) Y.E_{elec} + \frac{N}{C} Y + Y.E_{elec} + Y.\varepsilon f_s d_{CH}^2, \quad (5)$$

When applying the Euclidean distance formula, the size of each cluster will be equal to $\lambda = \frac{R^2}{C}$, where $\rho(x,y)$ represents the distribution of nodes within the cluster. If we consider that space is a circular shape with a radius of $\eta = R/\sqrt{\pi C}, \rho(r,\theta)$, and if the density ρ is constant at all points, with a uniform density of $\rho = (\frac{1}{\frac{R^2}{C}})), d_{CH}^2$, then the expression for d2CH can be simplified in the following manner:

$$d_{CH}^2 = \int\int (x^2 + y^2)\rho(x,y)dxdy = \int\int r^2 \rho(r,\theta) r dr d\theta, \quad (6)$$

$$d_{CH}^2 = \int\int (x^2 + y^2)\rho(x,y)dxdy = \rho \int_{0=0}^{2\pi} \int_{r=0}^{R/\sqrt{\pi C}} r^3 dr d\theta = \frac{R^2}{2\pi C}, \quad (7)$$

The amount of energy lost in a group during each rotation. The energy dissipation of each cluster will be added together, and the overall amount of energy used in the network for each round will equal the combined energy consumption of all clusters. This means that the amount of energy used by each cluster will be combined. To find ideal number of created clusters, one can calculate the derivative of E_{tot} for C and set it equal to zero. The typical distance between a CH and BS, known as d_{BS}, can be expressed as $A = R^2/R1$. If a large proportion of nodes are more than d0 away from the BS, after conducting a similar analysis. By replacing the value in Equation (9) and taking the derivative of E_{tot} in terms of C and setting it equal to zero, we can determine:

$$E_{cluster} \approx E_{CH} + \frac{N}{C} E_{nonCH}, \quad (8)$$

$$E_{tot} = CE_{cluster} = Y(N(1 + E_{elec}) + C\varepsilon f_s d_{BS}^2) + NL(E_{elec} + \varepsilon f_s d_{CH}^2), \quad (9)$$

$$C_{opt} = \sqrt{\frac{NL}{2\pi Y}\frac{R}{d_{BS}}} = \sqrt{\frac{NL}{2\pi Y}\frac{2}{0.765}}, \quad (10)$$

$$d_{BS} = \int \sqrt{x^2 + y^2}\frac{1}{A} dA = 0.765\frac{R}{2}, \quad (11)$$

$$E_{CH} = \left(\frac{N}{C} - 1\right) Y.E_{elec} + \frac{N}{C} Y + Y.E_{elec} + Y.\varepsilon_{mp} d_{BS}^4 \quad (12)$$

$$C_{opt} = \sqrt{\frac{NL}{2\pi Y}}\sqrt{\frac{\epsilon fs}{\epsilon mp}}\frac{R}{d_{BS}^2}, \quad (13)$$

The ideal likelihood for a node to become a CH, p_{opt}, can be calculated in the following manner:

$$p_{opt} = \frac{C_{opt}}{N}, \quad (14)$$

Identifying the optimal probability of a node being CH is equally significant as determining the proper formation of clusters. The groups do not form the optimal path, the total energy consumed by the WSN increases in each round. This is especially true when the number of clusters created deviates from the ideal number - more or less. If a smaller number of clusters are created, some nodes in the network must send their data over long distances to reach the CH, which increases the energy consumption. On other hand, if there are more clusters than necessary, this may lead to reduced routing traffic within each cluster due to fewer members. However, having more clusters also means that there will be more one-hop transmissions from CHs to BS and less data aggregation being performed within each cluster, leading to increased communication among CHs.

3.3 Cluster-based Routing Model:

Once the clusters have been formed, the cluster leaders must transfer their accumulated data to the central node. This requires the implementation of an inter-cluster routing protocol. Communication power is the main drain on power in wireless networks, and it has a significant impact on communication distance. Therefore, utilizing the shortest path can greatly reduce energy consumption. However, it is possible that this approach may not effectively extend the network's lifespan. To achieve energy-efficient routing, there must be a balance in energy usage within the network. Relying solely on the remaining energy of sensor nodes is not an optimal method for achieving this balance. The routing protocol must not require high traffic and low power nodes to be washed after installation. By introducing a new recommendation function—the energy load function—which considers the balance of energy and traffic load of the sensor nodes, we can significantly influence the selection of soap nodes. The number of messages sent by each cluster head is proportional to the number of members and other cluster heads for transmission purposes. This means that a relay node should be chosen based on higher energy levels and lower load. Equation (15) outlines our proposed relay energy metric for cluster head y at time t.

$$REM_y(t) = \exp\left(\frac{RE_y(t)-(NDR_y(t)*HE_{xy})}{IE_y}\right) \qquad (15)$$

Determine the single-hop transmission capacity from $x\ to\ y$, which is equivalent to HE_{xy} and determines the CH Y is found. The energy consumption of the cluster head is quantized into a new energy function by equation (15) after all messages have been sent. Modifying the input to the coding process can cause significant changes in the output. By using the exponential function, even a small change in the energy levels of the nodes can determine the relay node with the maximum energy consumption. In ERCP, each group head collects data from its member units and evaluates neighboring group heads on a cost basis to determine the best one. Data is then sent to the synchronization node from this specific neighbor. Connection quality, power measurements, and distance to the synchronization node are among the parameters used to calculate the cost function. The node with a high-power measurement value should function as a relay node to ensure equal power consumption. Additionally, the use of a short-distance node can decrease energy usage and transmission delay. You can also prevent unreliable connections by selecting the node with optimal connection quality. The cost for cluster head x to select cluster head y as a relay node is as follows:

$$RCost_{xy}(t) = \left(REM_y(t) + \frac{1}{ED_{(y,sink)}}\right) * PRR_{xy}(t) \qquad (16)$$

In equation (16), ERCP inter-cluster routing algorithm 1 is presented, which selects the relay node from its available options by using the cluster head with the highest cost and value.

Algorithm 1: ERCP-Next-Hop-Selection Algorithm

Input: = $Relay\ node\ ID;\ Y\ =\ Next\ relay\ node;\ next_{hop}[] = Array\ containing\ the\ selected\ relay\ nodes;$

Output: $X\ =\ The\ number\ of\ neighbors\ located\ in\ the\ direction\ of\ sink\ node;$ $P[X] = Array\ for\ sorting\ probability\ amount\ of\ nighbors;$
$Node\ x\ sends\ “next\ hop\ selection\ message”\ to\ its\ cluster\ head\ neighbors\ NEB_x;$

```
Each node $y \in NEB_x$ sends reply with the current $RE_y(t), PRR_{xy}(t), NDR_y(t)$;
For each $y \in NEB_x$ do
    If $((ED_{(y,sink)} \geq ED_{(x,sink)} | y \in next\_hop[]))$
        Discard the reply message;
    Else
        Calculates the cost $RCost_{xy}(t)$ of each $y$ based on Equ (15) and equ (16);
```

```
                $P[] \leftarrow RCost_{xy}(t);$
            $End\ if$
$End\ for$
$P_{max} = 0;$
$for\ (r = 0; r = X; r++)$
    $If\ (P[r] > P_{max})$
        $P_{max} = P[r];$
        $x = y.P_{max};$
        $next\_hop[] = y$
    $End\ if$
$End\ for$
$End\ Proc$
```

3.4 Trust Analysis:

3.4.1 Direct Trust Analysis

In this part, the assessment of Direct Trust for communication within a cluster (SD and CH) and between CH to CH and CH to BS is discussed. By using $L_o^u(x,y)$, one can determine that the sensor unit x and the associated sensor units have reasonable trust in each other after at least some initial interaction in the uth session. The Direct Trust is calculated using the trustable metric according to the equation below.

$$L_o^u(x,y) = Sec_o^u(x,y). \qquad (17)$$

Provided that the sensor unit y has an improved transmission function as per Eq (17). The parameter x of the sensor device is highly reliable. This helps the sensor device y obtain a more dependable parameter from $x's$, from the viewpoint of the sensor device.

3.4.2 – Indirect Trust Analysis

This chapter covers the indirect assessment of in-person and telephonic communication, considering insights from traditional musical instruments. To ensure communication, the cell unit requests feedback from other cells about its actions. The collected feedback from other sensors is then combined to calculate the Indirect Trust score using the following formula.

$$G_o^u(x,y) = \begin{cases} \frac{\sum_{p \in Z-\{x\}} F_o^u(x,p) * L_o^u(x,y)}{\sum_{p \in Z-\{x\}} F_o^u(x,p)}, & if\ |Z - \{x\}| > 0, \\ 0, & if |Z - \{x\}| = 0. \end{cases} \qquad (18)$$

In this context, Z represents the collection of $S(y)$ and y, which refers to the sensor device that has been in contact with the sensor devices.

3.4.3 – Recent Trust Analysis

This portion introduces a Contemporary Trust analysis of communication within a cluster and between clusters in heterogeneous WSNs. The ultimate reliability factor can be determined by utilizing both direct and indirect measures of reliability. In this case, direct reliability is better because the data sensor device has a higher level of interaction with the fixed sensor device. At sensor unit x, the confidence factor for the current measurement is $C_o^u(x,y)$ at the time of measurement. The value of the reliability factor is denoted by the letter δ in this equation.

$$C_o^u(x,y) = \delta * L_o^u(x,y) + (1-\delta) * G_o^u(x,y) \qquad (19)$$

The variable $T^u(x,y)$ represents number of times that the sensor device x interacts with the sensor device y during the uth session. Similarly, $\vec{T}^u(x,y)$ represents the average size of interactions initiated by other sensor devices towards sensor device y. This is calculated using the equation below.

$$\vec{T}^u(x,y) = \frac{\sum_{p \in Z-\{x\}} F_o^u(x,p) * T^u(p,y)}{|Z-\{x\}|} \qquad (20)$$

3.5 Distributed Compressive Sensing Technique (DCST)

3.5.1 – Compressive Sensing Process:

Signals with low or compressibility can be modeled as compressive sensing, where a set of linear projections is used to reconstruct sparsely transmitted signals. For example, a sparse signal is one with naturally few non-zero elements, while if converting the nature of such compressible signals into another space with minimal energy conservation, they can be represented as sparsely equivalent by using this technique. Assuming a sparse representation in some form of Fourier or Wavelet basis, let $X \in R^N$ be characterized as a discrete signal with a corresponding $N \times 1$ column vector, and use the following mathematical expression for compressive sensing. By assuming a sparsity, the signal can be expressed in terms of the basis that is chosen. It is stated that on an orthonormal basis,$N \times Northonormal\ basis\ matrix\ \Psi = [\Psi_1, \Psi_2, \ldots\ldots, \Psi_N], \Psi_k,\ \ k = 1,2, \ldots, N\ is\ a\ N\ 1 vector, and\ a = [a_1, a_2, \ldots, a_N]$. This vector is represented by the matrix $(K < M \ll N)$ in the Ψ domain. A signal, denoted as can be considered compressible or sparse on this basis if its coefficient vectors have mostly small or zero elements with only a few large ones. Most elements are free, to put it simply. According to the recognition theory, if the signal is K-sparse, it can be captured and recovered under certain restrictions from non-integral linear measurements of M. The signal is modelled by CS as follows:

$$X = \sum_{k=1}^{N} a_k \Psi_k = \Psi a \qquad (21)$$

$$Y = \varphi X \qquad (22)$$

In this scenario, represents a measurement matrix where $Y = [y_1, y_2, .., y_M]$ is $M \times 1$ are its elements. Correspondingly, $\varphi = [\varphi_1, \varphi_2, \ldots, \varphi_M]$ is an N×1 sensor matrix with $\varphi, i = 1,2, \ldots N$ elements. Each element of the sensor array is the product of the vector X and the vector φ_i. The second principle can be viewed as the randomness of the measurement matrix, which should be considered. By replacing X with Ψa, y can be rewritten as:

$$Y = \phi X = \phi \Psi a = \Theta a \qquad (23)$$

RIP can be used to reconstruct the scattering profile using M measurements, as proposed by the theory of strain induction. Due to this characteristic, the matrices $\phi\ and\ \psi$ have minimal overlap, which implies that rows of minus are not to be confused with columns of less than Ψ, but vice versa. Whenever the smallest number in the matrix Θ of order $\delta_k \epsilon (0,1)$ can satisfy the condition of RIP, it is always $M\ \times\ N$. This isometric coefficient (RIC), For all values of $||a||_0 \le K, and\ ||a||_0$, equation (24) must be satisfied. l_0 is the method for determining the number of non-zero elements in a range of l_p.

$$(1 - \delta_k)|||a|_p^p \le |||\Theta a|_2^2 \le -(1 + \delta_k)||a||_2^2 \qquad (24)$$

$$||a||_p^p = \sum_{i=1}^{N} |a_i|^p \qquad (25)$$

$$M \ge cKlogN/K \qquad (26)$$

Although it is a difficult task, the signal l_1 can be retrieved from through optimization. The most used method for reconstructing CS signals is l_0 minimization, but l_1 minimization is too complex to compute. The coefficients of the scattering signal a can be determined by solving for l_1 minimization.

$$X = \Psi a;\ \ a = \arg\ \ min_{a \epsilon R^N} |||a||_{l_1}\ \ \ s.t.\ \ Y = \phi X \qquad (27)$$

3.5.2 – DCST-based Common Part Recovery

Our suggested method, which relies on belief propagation, employs the use of factorial diagrams is common in the creation of a graphical representation model for this model. Before describing the graph, we must first determine the probability distribution of the factor elements to be included in the factor graph. We can say that $P(s_i = 1) = \beta$ and that every shape variable follows a Bernoulli distribution. Assuming that the signal K is spread, $\beta = K/N$ can be set. As a result, the prior probability distribution for each character variable can be expressed as:

$$p(s_i) = \begin{cases} \beta = \frac{K}{N} & s_i = 1 \\ 1 - \beta = 1 - \frac{K}{N} & s_i = 0 \end{cases} \qquad (28)$$

Variable nodes (VN), connected nodes (CNs), and edges (Es) are the building blocks of a bipartite graph, which is represented by $G = (VN, CN, E)$. The problem's nature permits us to compute the probability distribution with ease, as explained in the previous section. The construction of this graph involves connecting variable nodes and link node edges that are not directed when a variable node relies on underlying data. Messages exchanged between variables and connection nodes can be utilized to calculate side distribution functions in this manner. Two subgraphs in VN_2, nests, have the coefficient $\{z_i\}$ to multiply. The first subgraph (sub-graph 1) is responsible for plotting the marginal posterior distribution $\{z_i\}$. A good solution can only be obtained by selectively selecting the appropriate probability distribution functions. By approximating the signal elements, subgraph 2 provides an appendix that indicates the level of signal dispersion. Two variable nodes and a connection node, where the shape variables VN_1 and the symbol variables are considered variable Nodes. One example of this, with CN_1, which represents underlying nodal relationships between state variables and symbolic elements. By using the belief propagation method, the connection node's edges and index coordinates are used to provide information about the estimated index coordinate values on this graph. This information is used to update our estimate of the level of symptom spread. Therefore, VN_1 gives the distribution of each state variable $p(s_i)$. The Gaussian distribution of z_{ik} can be found by reducing the point elements using shape variables, as shown in CN_1. The next step is to establish the boundary between each connection node and each variable point, which can be done by the following methods:

$$CN_1(z_{ik}, S_i) \sim p(z_{ik}|S_i) \qquad (29)$$

$$\mu_{CN_1 \to Z}(z) = \sum_{\sim(z)} CN_1\big(N(CN_1)\big) \qquad \prod_{v \in N(CN_1)\{Z\}} \mu_{v \to CN_1}(v) \qquad (30)$$

All the variable nodes associated with CN_1 are denoted by the constant value of $N(CN_1)$ for each number, while - represents the sum of all variables except z. The boundaries of the connection node CN_1 and variable nodes are denoted by a label: $\mu_{v \to CN_1}(v)$. In terms of the prevalence of belief, these boundaries represent the degree to which the belief is a common descriptor. There are two Gaussian distributions for the zero and non-zero coefficients of the signal. VN_2 is used to pass the parameters and compute the mixed Gaussian distribution for the point elements, which is determined by arithmetic constant (CN_1) in vector geometry. VN_2 is used to calculate the prior probability distribution of z_{ik} after these parameters have been determined. Given that the $a\ Diarac\ distribution\ function\ and$ The function $\delta(x)$, where [l] for $\int \delta(x)dx = 1$ represents its derivative. In this design, the customer has a chance. On the right, the second binary graph has two variable nodes and one connected node: VN_2, which is shared with sub-graph 1. The connecting node is defined as a pair of metric variables, with VN_3 and at least two other values being used to represent the variable nodes. This subgraph is responsible for determining the edge distribution of the point elements. This distribution can be done by multiplying all received messages by different nodes. Extracting the input edges from the variable node VN_2 is done only on nodes in the hierarchy, such as nod 0 and nodule n. The edges present details about the status of the symbolic elements for the connected node. A combination of Gaussian densities is present in the input edges. Gaussian density is transmitted between all nodes involved in the measurement, with each member node VN_2 sending its value. CN_2 is a delta function node that links the signal observation variable nodes - VN_3 and – in particular, between the signals observed by two receivers. This connection node is defined as follows:

$$p(z_{ik}|s_i) = \beta \times p(z_{ik}|s_i = 0) + (1 - \beta) \times p(z_{ik}|s_i = 1) = \beta \times (\mu_1, \sigma_1^2) + (1 - \beta) \times N(\mu_0, \sigma_0^2) = \beta \times N(\mu_1, \sigma_1^2 + (1 - \beta) \times \delta((Z_{ik}) \qquad (31)$$

$$CN_2(z) = \prod_{u \in N(z)} \mu_{u \to z}(z) \qquad (32)$$

$$CN_2(Z^k, y_{ik}) = \delta(y_{ik} - \sum a_{ik} z_{jk}), \qquad z_{ik} \epsilon Z^k \qquad (33)$$

$$P(z_{ik}|Y) = CN_{ik}(Z^k, y_{ik}) \times \prod_{i \neq j} \mu_{zjk \to ZYik}(z_{jk}) \qquad (34)$$

$$p(Z^k|Y) = \prod_{i \neq j} p(z_{ik}|Y) \qquad (35)$$

A delta node junction function is utilized to compute the marginal distribution for all variables, by multiplying the value of the variable z_{ik} with the other density functions of each variable node y_{ik}. Convergence is achieved by computing the marginal distribution at each convergence stage of an algorithm. By assuming that the signal coefficients are not related, we can determine the connected distribution of the given signal Z. Therefore, all input Gaussian denies are gathered by every connection node, and they are calculated as a product of the number of input connections to that node. A support set for an indicator is identified in the second section of the chart, which serves as its primary purpose. This involves determining the posterior distribution of the state variables at the synchronous node based on the sensor reading, which is done by calculating the likelihood ratio specified below. If this function is expressed as z_{ik}, then it should also be possible to divide this likelihood ratio into smaller parts.$VN_3 = Y$ are the two distinct nodes in this diagram, with each having a connection point that corresponds to another node. Every time that the algorithm is executed, the variable nodes $VN_3 = Y$ send their marginal distribution values to the variables whose value is zero on the matrix. The Gaussian density is computed by multiplying the input edges with multiple messages using the variable node VN_2in equation (31). This function's parameters are conveyed to the connection node by connecting a pair of connections concerning each other, such as the variable nodes $VN_3 = Y$ and VN_3 and VN_4. As the preceding likelihood ratio is mentioned, these edges become the second parameter. The connection node calculates the first part of this ratio CN_3 by considering the Bayesian rules and the prior probability distribution. Link node members are linked to the token elements under the following support pattern:

$$SSet = \left\{ \frac{i}{;\frac{p(S_i = 1|Y)}{p(S_i = 0|Y)}} \geq 1 \right\} \tag{36}$$

$$\frac{p(s_i=1|Y)}{p(s_i=0|Y)} = \frac{\int p(s_i=1|Y,z_{ik})p(z_{ik}|Y)}{\int p(s_i=0|Y,z_{ik})p(z_{ik}|Y)} \tag{37}$$

$$CN_3(|SSet|,Z) = p(|SSet||Z) = \frac{P(Z||SSet|)\times P(|SSet|)}{P(Z)} \tag{38}$$

By denoting $|SSet|$ and its cardinality by index K, the set of supported identifiers is retrieved. Due to the higher ratio than the dispersion level K, it is crucial to reduce the cardinality. Although $p(|SSet||Z)$ has been calculated in equation (31) previously, there are $R = \binom{N}{K}$ sets that can be used as support sets, with K representing the number of zeros. -zero -elements in the support set There are K non-zero elements in the support set, so there are $\binom{N}{K}$ ways to choose the support set. We define $RSet = \{PSSet_1, PSSet_2, \dots., PSSet_k\}$ as the set of all possible support sets with cardinality K, but $(\overline{RSet})$ denotes the non-all collections may be included. support package to find $P(Z||SSet|)$, we need to compute two marginal distributions: one for the nonzero elements of each support set $PSSet_i$ and one for the nonzero elements of $\overline{PSSet_\iota}$ (non-supportive set). The marginal distribution for elements in $PSSet_i$ is computed using the Gaussian distribution provided by $p(Z_{ij}|s_j = 1)$, with the value of p being determined for each element of $(\overline{PSSet_\iota})$, and the values of both SDSS and PSA are presented. For each possible support set, the connected node CN_3 multiplies the marginal distributions of these elements to obtain the following probability:

$$p(Z^k||PSSet_i|) = \prod_{i\epsilon PSSet_i} p(Z_{ik}|s_i = 1) \times \prod_{j\in PSSet_i} p(Z_{jk}|s_j = 0) \tag{39}$$

$$p(Z^k||SSet|) = \sum_{i=1}^{\binom{N}{K}} p(z^k||PSSet_i|) \tag{40}$$

In conclusion, the connection node CN_3 combines and includes all these marginal distributions for all members. Since each potential support set has an equal chance of being the main support set, the value of $P(|SSet| = 1/N$ can be represented as $P(Z^k)$. This can be determined using Equation (30). The transfer of $p(z^k||SSet|)$ and $p(z^k|Y)$ from connection node CN_3 to index nodes $SSet$ takes place. This variable node calculates the posterior distribution which is determined as follows:

$$p(|SSet||Y) = \sum_{zik} \sum_{z2k} \sum_{zNK} (p(|SSet||z^k) \times \prod_{i=1}^{N} p(z_{ik}|Y)) \tag{41}$$

These chances are traded for a set number of repetitions. Once completed, these component distributions are employed by Equation (36) to determine the optimal support set for the sink node. The process is resumed by the base station once it has identified and selected the most suitable support set. By using the $SSest$-defined support set, it retrieves the prior distribution of the benchmarks. The Z signal is reconfigured through the continuous exchange of probability functions between VN_2 and VN_3 and CN_2, which is used to determine marginal probabilities. Figures 2 and 3 represent the Factors graph representation, for an individual part, and algorithm 2 provides a DCST propagation for sparse signal recovery to achieve optimal recovery in resource-constrained networks like WSNs.

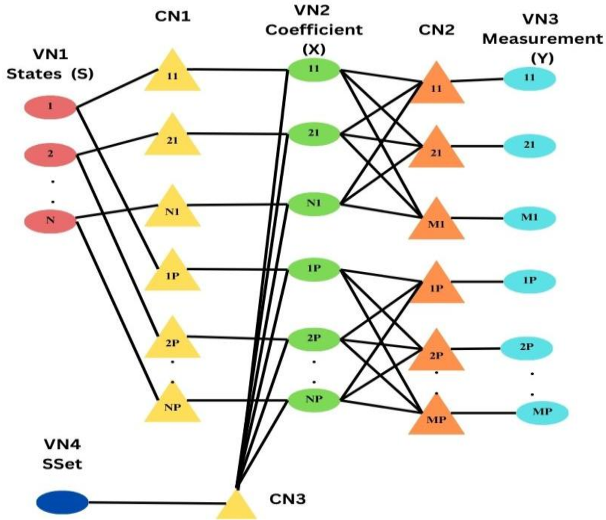

Figure 2 - Factor graph representation

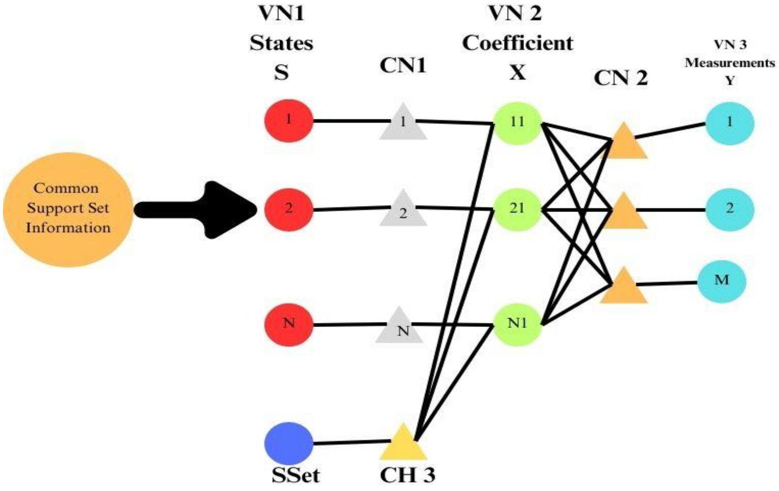

Figure 3 - Provide a factorial diagram for the same element.

Algorithm 2 – DCST with belief propagation

Input: X, discrete signal represented as an $N \times 1$ vector. $\Psi - N \times N$, orthonormal basis matrix. Φ, measurement matrix $M \times N, where\ M \ll N$. Sparsity level K and desired error tolerance.

Output: Compressed signal Y, recovered signal coefficient a, and posterior distribution $p(|SSet||Y)$.

The signal X as a sparse representation in terms of the chosen basis Ψ

Compute $X = \Psi a$, where $a = [a_1, a_2 \dots, a_N]$ is the sparse coefficient vector.

```
    Compress $X$ using measurement matrix $\phi$, $Y = \phi X = \psi a = \Theta a$.
    Ensure Θ satisfies RIP, allowing recovery of X using M, $(1-\delta_k)|||a|_p^p \leq |||\Theta \mathrm{a}|_2^2 \leq -(1+\delta_k)||a||_2^2$.
    Initialize factor graph $G = (VN, CN, E) with\ variable\ nodes$ V N, connected nodes CN, and edges E.
    For variable nodes $s_i\ in\ \Psi$, $p(s_i) = \begin{cases} \beta = \frac{K}{N} & s_i = 1 \\ 1 - \beta = 1 - \frac{K}{N} & s_i = 0 \end{cases}$, establish connections between VN and CN
nodes to form the bipartite graph.
        For each $z_{ik}$ and shape variable $s_i$, compute Gaussian distribution on $CN_1$, $CN_1(z_{ik}, S_i) \sim p(z_{ik}|S_i)$.
    Update distribution with message $\mu_{CN1} \to z(z)$, $\mu_{CN_1 \to Z}(z) = \sum_{\sim(z)} CN_1(N(CN_1)) \quad \prod_{v \in N(CN_1)\{Z\}} \mu_{v \to CN_1}(v)$
Identify support set $SSet$ by likelihood ratio, $SSet = \left\{ \frac{i}{; \frac{p(S_i = 1|Y)}{p(S_i = 0|Y)}} \geq 1 \right\}$
Support set, reconstruct the signal, $X = \Psi a$.
The recovered signal X and posterior probability $p(|SSet||Y)$
End
```

4. SIMULATION ENVIRONMENT

The Ubuntu OS software ns3 is an integrated network of interconnected devices that can automatically exchange data and perform tasks. The languages used in the implementation of Ns3 are C++ and Python. C++ is the programming language used for front-end and network construction, while Python is used in analysis and back-end processing. Some of the input parameters considered for this analysis are listed in the final calculated results compared to CACIACA [29], OCCMPHE [30], EMRHPFC [31], and ELRC-DCS.

4.1 Communication Delay: The sender to the receiver in the network is known as communication latency. The factors that are considered include delivery, generation, processing, and queuing time. Understanding and reducing communication latency is critical to increasing the performance and responsiveness of network applications. Fig 4, shows the communication delay compared ELRC-DCS model with other existing models.

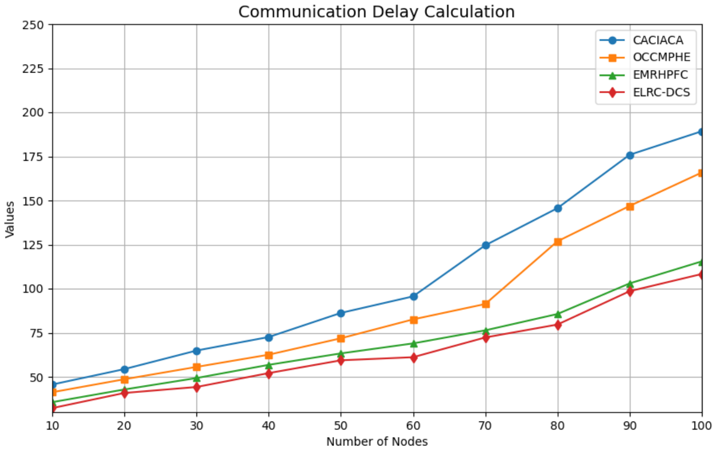

Figure 4 - Communication Delay Calculation

4.2 Energy Efficiency Calculation: Efficiency in energy usage involves utilizing less energy to accomplish the same task and achieve an identical output, leading to lower overall energy consumption and waste. Technology and networks require process optimization to achieve optimal energy efficiency and performance. To achieve stability and reduce operating costs, energy efficiency is crucial in applications such as computing and telecommunications. Fig 5, the ELRC-DCS model has been compared with other existing models.

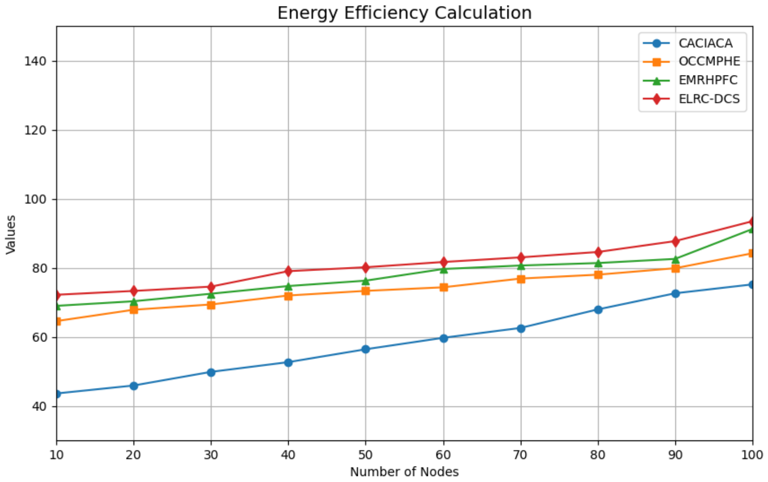

Figure 5 - Energy Efficiency Calculation

4.3 Data Success Rate: The success ratio of data packets or messages in a communication system is the measure of total number of packets sent. The efficiency and dependability of data transmission are evaluated by examining factors like packet loss, errors, and retransmissions. The success rate of data is a measure of the strength and accuracy of an information system. Optimizing network performance and maintaining high-quality service in various applications requires monitoring this speed. Fig 6, data success rate has compared the ELRC-DCS proposed model with another existing model.

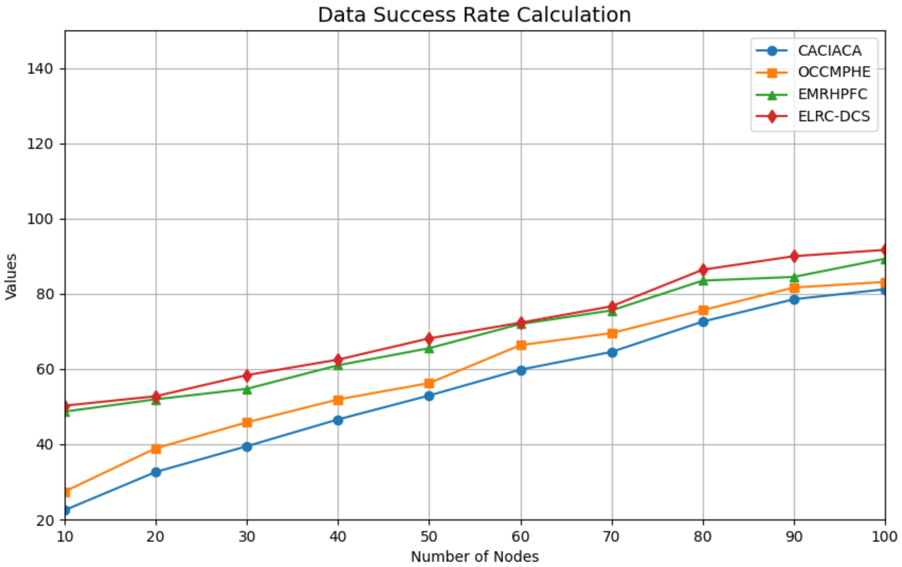

Figure 6 - Data Success Rate Calculation

4.4 Network Throughput Calculation: The rate of data transfer from one location to another on a network is called network throughput, measured in bits per second. It indicates the actual transfer rate bandwidth and factors such as network load, latency, or protocol overhead. Improved network performance, faster data transfer, and a better user experience are the benefits of increased throughput in applications like gaming consoles or streaming services. Improving network access is essential to meet the needs of large-scale applications and ensure efficient use of resources. Fig 7, network throughput compared with the ELRC-DCS proposed model with other existing models.

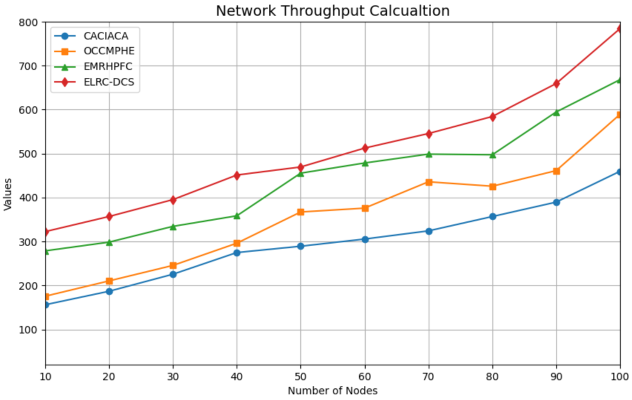

Figure 7 - Network Throughput Calculation

4.5 Routing Overhead Calculation: The overhead of routing affects the resources used by routing protocols to manage and maintain network paths, including bandwidth and processing power. The process involves exchanging routing information, maintaining, and storing routing tables, and devising calculations to identify the optimal routes for data transmission. Routing that is advanced can lead to a higher latency and subsequently, lower throughput on the network. Fig 8, routing overhead has compared with ELRC-DCS proposed model with other existing models.

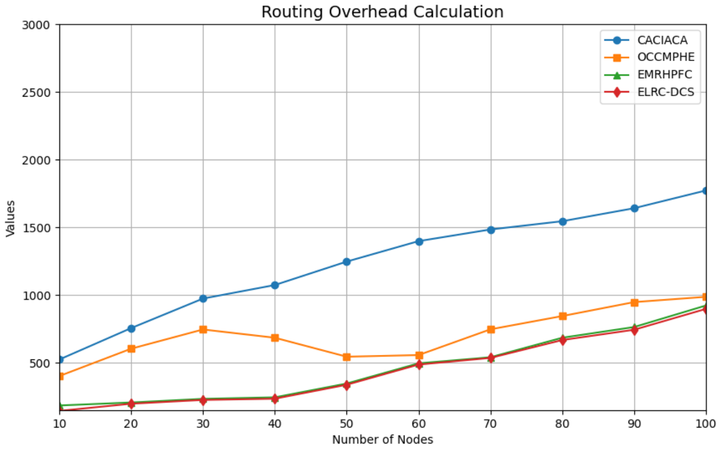

Figure 8 - Routing Overhead Calculation

5. RESULT AND DISCUSSION:

The ELRC-DCS protocol and the proposed model both demonstrate exceptional performance improvements in WSNs through optimized clustering and routing strategies that emphasize energy efficiency, low latency, and high data success rates. Fig 4, communication delay ELRC-DCS achieves the lowest latency at 108.30 ms, significantly outperforming other models like CACIACA at 189.24 ms and OCCMPHE at 165.85 ms. EMRHPFC model achieves 115.46 ms thus enhancing responsiveness for time-sensitive applications. The proposed model complements this by establishing the shortest, energy-efficient routes between CH and the sink, further reducing delay. Fig 5, energy efficiency with ELRC-DCS achieving 93.45% efficiency. CACIACA AT 75.16 %, OCCMPHE AT 84.17 %, AND EMRHPFC T 91.19 %. The proposed model maintains energy balance by rotating CH roles, thereby preventing premature battery depletion among individual nodes. This CH rotation and balanced cluster size also optimize energy usage, aligning with the ELRC-DCS's approach and resulting in an extended network lifespan. Fig 6, the data success rate ELRC-DCS outperforms with 91.64%, CACIACA AT 81.17 %, OCCMPHE at 83.12 %, AND

EMRHPFC at 89.28 % indicating reliable data transmission with minimal errors. Similarly, the proposed model enhances reliability through direct and indirect trust measures, which reduce low-quality data transmissions, ensuring dependable communication. Fig 7, network throughput of ELRC-DCS at 784.26 Kbps CACIACA at 459.78 Kbps, OCCMPHE at 589.28 Kbps, and EMRHPFC at 668.17 Kbps demonstrates its high data handling capacity, a significant advantage for high-demand applications. The proposed model supports efficient data handling by utilizing the DCST to compress data, thus reducing packet volume and energy use while maintaining data fidelity. Fig 8, routing overhead with ELRC-DCS achieving the lowest at 898 packets, CACIACA at 1772 packets, OCCMPHE at 987 packets, and EMRHPFC at 923 packets facilitating faster routing and improved bandwidth usage. The proposed model's relay node selection mechanism, based on energy levels and load, further reduces routing complexity, contributing to enhanced network performance and longevity. ELRC-DCS and the proposed model represent robust solutions for WSN applications, offering comprehensive improvements in efficiency, reliability, and network durability, which make them well-suited for sustainable and time-sensitive applications. The overall comparison table is shown in Table 1.

Table 1 - Overall Comparative Performance Analysis

Parameters	CACIACA	OCCMPHE	EMRHPFC	ELRC-DCS
Communication Delay (ms)	189.24	165.85	115.46	108.30
Energy Efficiency (%)	75.16	84.17	91.19	93.45
Data Success Rate (%)	81.17	83.12	89.28	91.64
Network Throughput (Kbps)	459.78	589.28	668.17	784.26
Routing Overhead (Packets)	1772	987	923	898

6. CONCLUSION:

Energy consumption, network lifetime, data transmission efficiency, and security are among the critical issues that HWSNs face, which the proposed ELRC-DCS approach can address. Balanced energy usage across all sensor nodes is achieved through hierarchical clustering and energy-efficient multi-hop routing in the ELRC-DCS model, which can significantly extend the network's operational lifespan. By utilizing the energy balance, CH is used to select which loads to be balanced and maintain uniform energy usage throughout the entire network. Integration of DCST to decrease the amount of data being passed through it via the network. The reduction in communication expenses is achieved by enabling efficient data reconstruction from incomplete measurements, which reduces the energy consumption associated with transmitting excessive or redundant data. The ELRC-DCS framework employs compression to optimize network performance, even when resources are limited. The ELRC-DCS method incorporates a manual safety mechanism. HWSNs are particularly vulnerable to the transmission of data through multiple nodes, which can be easily hacked. By evaluating the direct, indirect, and updated trust values, this model ensures reliable communication between nodes and enhances the network's security. By enhancing data integrity, this approach safeguards against various security risks, including data manipulation and malicious node activity. Compared to traditional routing techniques in WSNs, the ELRC-DCS proposed model is highly effective and exhibits significant gains in energy efficiency, network lifetime, and data reliability. By using the ELRC-DCS approach, network longevity, and performance enhancement are achieved by reducing energy consumption per node, minimizing data transmission delays, and increasing the packet delivery ratio. Especially well-suited for large-scale environmental monitoring applications that require energy efficiency and data accuracy, the ELRC-DCS model is highly adaptable to this application. The ELRC-DCS model is designed to address various issues in HWSNs, including energy efficiency, load-balanced routing, compressive sensing, and security enhancements. By combining hierarchical clustering with multi-hop routing, compressive sensing, and trust-based security it is highly adaptable to different contexts of deployment for the HWSN. Further improvements to this model are possible through the integration of mobility support, improved accuracy of trust-based evaluations, and exploration of further compressive sensing techniques for handling higher-dimensional data. ELRC-DCS is an important step towards providing stable and low-power HWSNs in real life. The comparative analysis of the four models

CACIACA, OCCMPHE, EMRHPFC, and ELRC-DCS. With the lowest communication delay of 108.30 ms and the highest energy efficiency at 93.45%, ELRC-DCS demonstrates exceptional performance in enhancing network efficiency. Its superior data success rate of 91.64% and network throughput of 784.26 Kbps highlight its capacity to maintain robust communication under varying conditions. The minimum routing overhead required to optimize the resource usage is 898 packets. The ELRC-DCS model stands as a key solution for improving network performance, as it makes a significant contribution to network optimization.

Compliance with Ethical Standards:

- **Conflict of Interest:** The authors declare that they have no known competing financial interests or personal relationships that could have appeared to influence the work reported in this paper
- The authors declare that there was no participation of Human or Animal in the work reported in this paper
- Informed consent is not applicable for the work reported in this paper

REFERENCES:

[1] Ahmed M. Khedr, "Effective Data Acquisition Protocol for Multi-Hop Heterogeneous Wireless Sensor Networks Using Compressive Sensing", Algorithms, vol. 8, pp. 910-928, 2015, doi: 10.3390/a8040910

[2] Xin Cui, Xiaohong Huang, et.al, "A Load Balancing Routing Mechanism Based on SDWSN in Smart City", Electronics, vol. 8, pp. 273, 2019, doi: 10.3390/electronics8030273

[3] Chih-Min Yu, Mohammad Tala't, et.al, "Joint Balanced Routing and Energy Harvesting Strategy for Maximizing Network Lifetime in WSNs", Energies, vol. 12, pp. 2336, 2019, doi: 10.3390/en12122336

[4] Regonda Nagaraju, Venkatesan C, et..al, "Secure Routing-Based Energy Optimization for IoT Application with Heterogeneous Wireless Sensor Networks", Energies, vol. 15, pp. 4777, 2022, doi: 10.3390/en15134777

[5] Jun Yin, Yuwang Yang, et.al, "An Adaptive Data Gathering Scheme for Multi-Hop Wireless Sensor Networks Based on Compressed Sensing and Network Coding", Sensors, vol. 16, pp. 462, 2016, doi: 10.3390/s16040462

[6] Haifeng Zheng, Jiayin Li, et.al, "Spatial-Temporal Data Collection with Compressive Sensing in Mobile Sensor Networks", Sensors, vol. 17, pp. 2575, 2017, doi: 10.3390/s17112575

[7] Xiangping Gu, Xiaofeng Zhou, et.al, "A Data-Gathering Scheme with Joint Routing and Compressive Sensing Based on Modified Diffusion Wavelets in Wireless Sensor Networks", Sensors, vol. 18, pp. 724, 2018, doi: 10.3390/s18030724

[8] Ailian Jiang, Lihong Zheng, "An Effective Hybrid Routing Algorithm in WSN: Ant Colony Optimization in combination with Hop Count Minimization", Sensors, vol. 18, pp. 1020, 2018, doi: 10.3390/s18041020

[9] Ce Zhang, Ou Li, et.al, "A Practical Data-Gathering Algorithm for Lossy Wireless Sensor Networks Employing Distributed Data Storage and Compressive Sensing", Sensors, vol. 18, pp. 3221, 2018, doi: 10.3390/s18103221

[10] Fei Li, Min Liu, et.al, "A Quantum Ant Colony Multi-Objective Routing Algorithm in WSN and Its Application in a Manufacturing Environment", Sensors, vol. 19, pp. 3334, 2019, doi: 10.3390/s19153334

[11] Muhammad Bilal, Ehsan Ullah Munir, et.al, "Hybrid Clustering and Routing Algorithm with Threshold-Based Data Collection for Heterogeneous Wireless Sensor Networks", Sensors, vol. 22, pp. 5471, 2022, doi: 10.3390/s22155471

[12] Surjit Singh, Srete Nikolovski, et.al, "GWLBC: Gray Wolf Optimization Based Load Balanced Clustering for Sustainable WSNs in Smart City Environment", Sensors, vol. 22, pp. 7113, 2022, doi: 10.3390/s22197113

[13] Fatma H. El-Fouly, Ahmed Y. Khedr, et.al, "ERCP: Energy-Efficient and Reliable-Aware Clustering Protocol for Wireless Sensor Networks", Sensors, vol. 22, pp. 8950, 2022, doi: 10.3390/s22228950

[14] Neng-Chung Wang, Chao-Yang Lee, et.al, "An Energy Efficient Load Balancing Tree-Based Data Aggregation Scheme for Grid-Based Wireless Sensor Networks", Sensors, vol. 22, pp. 9303, 2022, doi: 10.3390/s22239303

[15] Mei Wu, Zhengliang Li, et.al, "A Dual Cluster-Head Energy-Efficient Routing Algorithm Based on Canopy Optimization and K-Means for WSN", Sensors, vol. 22, pp. 9731, 2022, doi: 10.3390/s22249731

[16] Divya Gupta, Shivani Wadhwa, et.al, "EEDC: An Energy Efficient Data Communication Scheme Based on New Routing Approach in Wireless Sensor Networks for Future IoT Applications", Sensors, vol. 23, pp. 8839, 2023, doi: 10.3390/s23218839

[17] Prakash Mohan, Vijay Anand Rajasekaran, et.al, "TPEMLB: A novel two-phase energy minimized load balancing scheme for WSN data collection with successive convex approximation using mobile sink", Ain Shams Engineering Journal, vol. 15, no. 10, pp. 102849, 2024, doi: 10.1016/j.asej.2024.102849

[18] R. Anto Pravin, K. Murugan, et.al, "Stochastic cluster head selection model for energy balancing in IoT enabled heterogeneous WSN", Measurement: Sensors, vol. 35, pp. 101282, 2024, doi: 10.1016/j.measen.2024.101282

[19] Kaviarasan R, Balamurugan G, et.al, "Effective load balancing approach in cloud computing using Inspired Lion Optimization Algorithm", e-Prime - Advances in Electrical Engineering, Electronics and Energy, vol. 6, pp. 100326, 2023, doi: 10.1016/j.prime.2023.100326

[20] Ansam ENNACIRI, Mohammed ERRITALI, et.al, "Load Balancing Protocol (EESAA) to improve Quality of Service in Wireless sensor network", Procedia Computer Science, vol. 151, pp. 1140–1145, 2019, doi: 10.1016/j.procs.2019.04.162

[21] S. Sandhiyaa, C. Gomathy, "A cross-layer approach for load balancing and energy-efficient QoS-based routing reliability for UWSN", Alexandria Engineering Journal, vol. 85, pp. 333–343, 2023, doi: 10.1016/j.aej.2023.11.019

[22] Gousia Thahniyath, Jayaprasad M, "Secure and load balanced routing model for wireless sensor networks", Journal of King Saud University – Computer and Information Sciences, vol. 34, pp. 4209–4218, 2022, doi: 10.1016/j.jksuci.2020.10.012

[23] Xu Dong Wen, Chun Wu Liu, "Decentralized Distributed Compressed Sensing Algorithm for Wireless Sensor Networks", Procedia Computer Science, vol. 154, pp. 406–415, 2019, doi: 10.1016/j.procs.2019.06.058

[24] G. Santhosh, K.V. Prasad, "Energy optimization routing for hierarchical cluster based WSN using artificial bee colony", Measurement: Sensors, vol. 29, pp. 100848, 2023, doi: 10.1016/j.measen.2023.100848

[25] Deepa Puneeth, Muralidhar Kulkarni, "Data Aggregation using Compressive Sensing for Energy Efficient Routing Strategy", Procedia Computer Science, vol. 171, pp. 2242–2251, 2020, doi: 10.1016/j.procs.2020.04.242

[26] Alireza Masoum, Nirvana Meratnia, et.al, "A distributed compressive sensing technique for data gathering in Wireless Sensor Networks", Procedia Computer Science, vol. 21, pp. 207 – 216, 2013, doi: 10.1016/j.procs.2013.09.028

[27] Lucia K. Ketshabetswe, Adamu Murtala Zungeru, et.al, "A compression-based routing strategy for energy saving in wireless sensor networks", Results in Engineering, vol. 23, pp. 102616, 2024, doi: 10.1016/j.rineng.2024.102616

[28] Vani S. Badiger, Ganashree T.S, "Data aggregation scheme for IOT based wireless sensor network through optimal clustering method", Measurement: Sensors, vol. 24, pp. 100538, 2022, doi: 10.1016/j.measen.2022.100538

[29] M. Shanmathi, Abhilash Sonker, et.al, "Enhancing wireless sensor network security and efficiency with CNN-FL and NGO optimization", Measurement: Sensors, vol. 32, pp. 101057, 2024, doi: 10.1016/j.measen.2024.101057

[30] Sharanu, Shivkumar S. Jawaligi, "ACRDA: An adaptive combined relay based dynamic data aggregation technique for wireless sensor networks", Measurement: Sensors, vol. 24, pp. 100571, 2022, doi: 10.1016/j.measen.2022.100571

[31] Lucia K. Ketshabetswe, Adamu Murtala Zungeru, et.al, "Energy-efficient algorithms for lossless data compression schemes in wireless sensor networks", Scientific African, vol. 23, pp. e02008, 2024, doi: 10.1016/j.sciaf.2023.e02008